Journal of Wind Engineering and Industrial Aerodynamics, 6 (1980) 73—88

COMPARISON OF MEASUREMENTS ON THE CAARC STANDARD TALL BUILDING MODEL IN SIMULATED MODEL WIND FLOWS

W.H. MELBOURNE

Department of Mechanical Engineering, Monash University, Clayton, Victoria 3168 (Australia)

(Received July 9, 1979; accepted in revised form November 13, 1979)

Summary

Measurements of surface pressures and response on the CAARC standard tall building model, made at six establishments, have been compared. In general, the degree of agreement was good and mostly within the scatter of reasonable experimental accuracy.

Small trends were observable in respect of pressure measurements which could be attributed to differences in the approaching longitudinal velocity spectrum and to the requirement for blockage corrections. There were no obvious trends in the dynamic response measurements where the majority of the data compared within ±15%.

1. Introduction

Following a meeting of the Commonwealth Advisory Aeronautical Research Council Coordinators in the Field of Aerodynamics in 1969, a specification for a "standard tall building model for the comparison of simulated natural winds in wind tunnels" was prepared by Wardlaw and Moss [1]. A simple model experiment was proposed for comparison between the techniques being established in various wind tunnels for the simulation of natural wind characteristics. It was hoped that direct comparison of the model dynamic response and pressure measurements would help in the development of better techniques and lead to more confidence in the considerable volume of test data being obtained from wind tunnel measurements.

In the period up to 1975, five centres undertook measurements on the CAARC Standard Tall Building Model. The work of the following people was made available to W.H. Melbourne, who made an initial comparison of the results for discussion at an evening meeting at the 5th International Conference on Wind Effects on Buildings and Structures, London, September 1975:

Holmes, J.D.,	The University of Western Ontario, Canada [2]
Lawson, T.V.,	University of Bristol, England
Melbourne, W.H.	Monash University, Australia
Walshe, D.E., Wills, J.A.B. and Jones, P.,	National Physical Laboratory, England [3, 4]

Cooper, K.R., and Wardlaw, R.L., National Aeronautical Establishment, Canada
Data were also presented by:
Sykes, D.M., The City University, England

It was agreed at that meeting that, after adjustments to achieve uniform presentation, a comparison of these results would be prepared, along with a commentary, so that other workers could "calibrate" individual techniques against this set of data relating to an isolated tall rectangular building.

2. Basic model specification

2.1 Building geometry

A rectangular prismatic shape was specified with full-scale dimensions, sides 100 ft by 150 ft and height 600 ft (30.48 × 45.72 × 183.88 m). The building was to be flat-topped, without parapets, and the exterior walls were to be flat without mullions or other geometric disturbances. Definitions of dimensions and angle of flow symbols are given in Fig.1 along with the location of surface pressure tap holes and numerical identification.

2.2 Dynamic properties of the building

Only the fundamental mode of vibration was to be considered and the mode shape was to be taken as being linear, rotating about a point at ground level. The natural fundamental frequency was to be taken as 0.2 Hz about both principle axes at ground level. The weight distribution was to be taken as 10 lb/ft^3 (density 160 kg m^{-3}). The structural damping was to be taken as being 1% of critical (logarithmic decrement 0.063) for purposes of comparison of results.

2.3 Wind structure

The natural wind boundary layer was to be representative of wind blowing over a long fetch of forest or urban development with building heights in the range of 20—50 ft (6—15 m). It was suggested that the power-law exponent for such a boundary layer would be about 0.28.

3 Model measurements

3.1 The natural wind models

The longitudinal mean velocity and turbulence intensity profiles, and velocity spectra of the seven adiabatic boundary layer wind models used for the tests reported are presented in Fig.2 and 3. The scale and methods used to develop the seven wind models are summarized in Table 1.

The differences between the mean velocity and turbulence intensity profiles are relatively small. The only significant differences between the seven wind models are in respect of the distribution of the turbulent energy as expressed by the longitudinal velocity spectra. In particular, the NPL wind model,

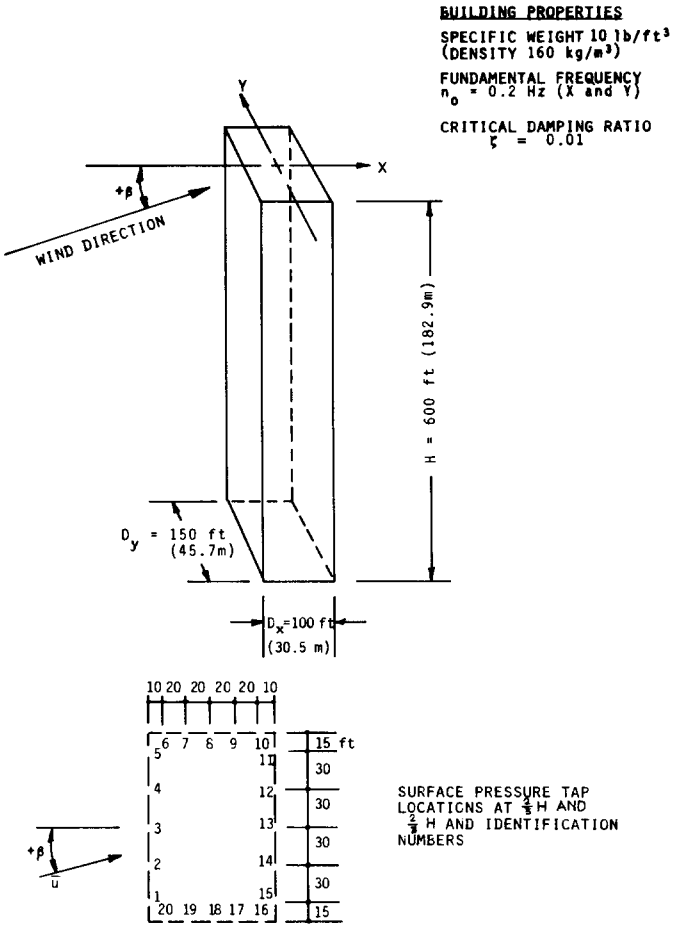

Fig.1. CAARC standard tall building: full-scale dimensions, dynamic properties and pressure tap locations.

has significantly more energy available at the resonant response frequencies through to the fine-scale end of the spectrum. It may be possible to detect the effect of this when comparing the response and pressure measurements at a later stage.

Blockage corrections have not been applied to any of the test data; model blockage as a percentage of working section area are noted in Table 1.

3.2 Pressure measurements

The mean and standard deviation of the pressures at $\frac{2}{3}H$ are given in Tables 2 and 3 for a range of wind directions 0 to 90° in 15° steps. In some cases, the participants in this exercise measured pressures at $\frac{1}{3}H$ and for a more extensive range of wind directions. However, for wind tunnel calibration purposes the range of data presented was thought to be adequate and also covered the

	VELOCITY PROFILE EXPONENT, α (where $\frac{\bar{u}_z}{\bar{u}_H} = \left(\frac{z}{H}\right)^{\alpha}$)	TURBULENCE INTENSITY AT THE TOP OF THE BUILDING, $\left(\frac{\sigma_u}{\bar{u}}\right)_H$
× CITY	0.23	0.08
△ BRISTOL	>0.3	0.10
+ MONASH	0.25	0.09
□ NAE (a)	0.28	0.09
○ NAE (b)	0.28	0.10
▽ NPL	0.25 to 0.3	0.085
○ WESTERN	0.28	0.10

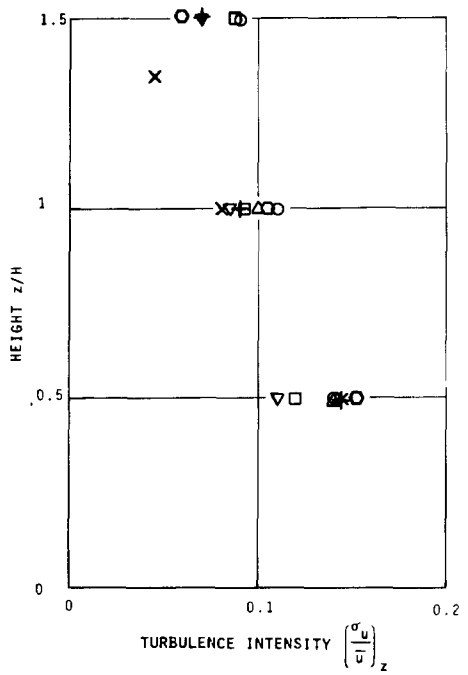

Fig.2. Longitudinal velocity profile and turbulence characteristics of the adiabatic wind models used for the CAARC building model tests.

best range for the purposes of comparing the five sets of data received.

In general, there is good agreement between the sets of data presented in Tables 2 and 3. There are several small trends which can be observed and for which there are possible explanations as follows:

1. The negative pressures from the City University measurements are lower (more negative) than the others, with the exception of those from NAE (b). This may be attributed to the model blockage which was between 3 and 4% and for which no corrections were made. From McKeon and Melbourne [5] the base pressure coefficient correction would have been between 0.10 and 0.13, which, if applied to the City University measurements, would provide good agreement with the other results.

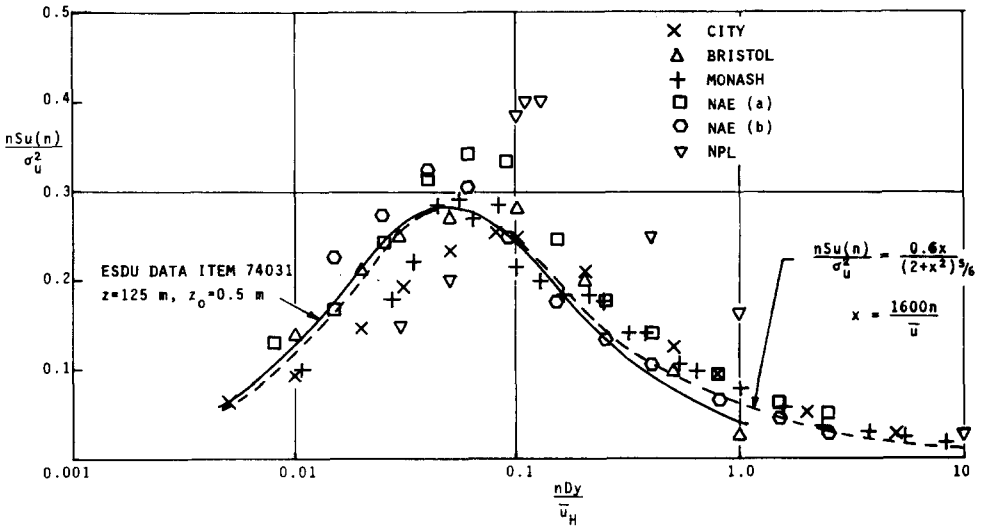

Fig.3. Longitudinal velocity spectra of the adiabatic wind models used for the CAARC building model tests measured at $z = \frac{2}{3}H$ (400 ft.).

2. The negative pressures from the NPL measurements are higher (less negative) than the others in spite of the model blockage being the second highest. This trend may be attributed to the higher turbulence available in the wind model at smaller scales, which is thought to reduce base pressures by promoting earlier re-attachment of the shear layers.
3. There is no obvious explanation for the lower (more negative) mean pressures from the NAE (b) measurements.

Pressure spectra were measured at Bristol, Monash, NAE and NPL, but unfortunately for a number of different conditions. The pressure spectra measurements most common to all are given in Fig.4. At Pressure Tap 3, for $\beta = 0$ the upstream face pressure spectra reflect the characteristics of the incident longitudinal velocity spectra, with NAE and NPL measurements showing higher energy at the higher frequencies relative to the Monash measurements. At Pressure Tap 13, for $\beta = 0$ the distributions of energy in the wake are shown to be similar, despite the differences in incident turbulence.

Measurements of mean, standard deviation and spectra do not describe all the relevant characteristics of pressures on buildings. A knowledge of peak pressures is most important for the design of cladding and glazing. A peak pressure may be related to the mean and standard deviation through the probability distribution of pressure. These probability distributions vary from being normally distributed to ones showing extremes of intermittency. Several examples of these pressure distributions, measured at Monash University, are given in Fig.5.

TABLE 1

C.A.A.R.C. BUILDING MODEL WIND TUNNEL AND MODELLING INFORMATION

Testing Establishment	Working Section Dimension (m)	Model Scale Parameters			Blockage ratio	Model Boundary Layer Development
		Length Ratio	Velocity Ratio for Building response measurements	Velocity for model pressure measurements m/s	Max. model area / working section area	
City University	0.76 x 0.60	$\frac{1}{690}$		15	3.9%	3 off 0.5 m high elliptic wedge vorticity generators and castellated barrier followed by a 1.6 m fetch of 17 x 17 x 20 mm high roughness elements in staggered array at 90 x 60 m centres.
University of Bristol	2 x 1	$\frac{1}{500}$	$\frac{1}{5}$	12	2.0%	Semi-elliptic wedge vorticity generators and 100 mm step followed by an array of 50 mm high cups.
Monash University	2 x 2	$\frac{1}{400}$	$\frac{1}{2.7}$	30	1.3%	4 off, 2 m high, 4° triangular vorticity generators followed by a 12 m fetch of 20 x 20 x 30 mm roughness elements.
National Aeronautical Establishment	9.1 x 9.1	$\frac{1}{400}$	$\frac{1}{4.5}$	15	0.06%	(a) 6 off 1.2 m high spires followed by 7.3 m fetch of 76 mm cube roughness elements on 0.3 m centres staggered array. (b) A 22 m fetch of 76 mm cube roughness elements on 0.3 m centres staggered array. (Note, spires are not used in this configuration.)
National Physical Laboratory	2.7 x 2.1	$\frac{1}{240}$	$\frac{1}{7.9}$	18.3	2.5%	Graded horizontal grid of 25.4 mm diameter rods, plus six 76 mm wide vertical slats. Model placed 3.7 m from grid, surrounded by roughness for approximately 1.5 m.
University of Western Ontario	2.4 x 2.1	$\frac{1}{500}$	$\frac{1}{4.5}$		0.6%	Graded grid of horizontal rods, 300 m high, followed by 25 mm cube roughness elements.

TABLE 2

C.A.A.R.C. BUILDING MODEL MEAN PRESSURE COEFFICIENT, $c_{\bar{p}} = \dfrac{\bar{p} - \bar{p}_H}{\frac{1}{2}\rho \bar{u}_H}$, AT Z = (2/3) H

Press. Tap / β	1	2	3	4	5	6	7	8	9	10	11	12	13	14	15	16	17	18	19	20	
0	0.59	.84	.87	.80	.54		-.76	-.77		-.84		-.55	-.53		-.61	-.84	-.82	-.82	-.79	-.75	City
	.49	.76	.80	.80	.53	-.66	-.69	-.70	-.73	-.77	-.58	-.51	-.50	-.53	-.59	-.76	-.71	-.70	-.70	-.66	Bristol
	.55	.78	.81	.78	.55	-.64	-.70	-.74	-.75	-.76	-.56	-.53	-.51	-.53	-.56	-.77	-.75	-.74	-.70	-.64	Monash
	.57	.81	.86	.84	.57	-.66	-.68	-.72	-.71	-.77	-.54	-.48	-.45	-.49	-.51	-.77	-.71	-.73	-.69	-.65	NAE (a)
	.54	.76	.81	.78	.49	-.85	-.85	-.88	-.86	-.66	-.66	-.62	-.58	-.59	-.66	-.64	-.90	-.91	-.86	-.86	NAE (b)
	.57	.76	.80	.76	.56	-.49	-.52	-.54	-.54	-.58	-.38	-.35	-.34	-.35	-.38	-.56	-.54	-.54	-.53	-.50	NPL
15	.64	.82	.79	.68	.38	-.56	-.58	-.59	-.64	-.65	-.51	-.51	-.53	-.54	-.51	-.55	-.72	-.99	-1.10	-1.07	City
																					Bristol
																					Monash
	.73	.88	.84	.77	.43	-.47	-.48	-.51	-.54	-.58	-.44	-.43	-.44	-.45	-.43	-.47	-.67	-.89	-.97	-.92	NAE (a)
	.66	.80	.75	.68	.44	-.37	-.38	-.38	-.40	-.44	-.32	-.32	-.33	-.34	-.34	-.38	-.56	-.79	-.92	-.89	NPL
30																					City
	.86	.83	.71	.53	.20	-.46	-.47	-.48	-.50	-.52	-.44	-.43	-.43	-.44	-.43	-.23	.04	.01	-.01	-.47	Bristol
	.80	.79	.66	.44	.23	-.48	-.49	-.51	-.51	-.52	-.43	-.45	-.45	-.42	-.39	-.18	.0	-.04	-.22	-.47	Monash
	.87	.82	.72	.53	.24	-.40	-.42	-.44	-.45	-.48	-.40	-.41	-.41	-.39	-.38	-.15	.0	.07	-.02	-.36	NAE (a)
	.79	.74	.65	.51	.25	-.35	-.35	-.36	-.36	-.37	-.32	-.32	-.33	-.34	-.34	-.12	.0	.08	.03	-.30	NPL
45																					City
																					Bristol
																					Monash
	.78	.61	.46	.30	.03	-.40	-.41	-.43	-.44	-.45	-.46	-.45	-.45	-.42	-.41	.01	.25	.39	.51	.67	NAE (a)
	.72	.54	.57	.20	-.06	-.54	-.55	-.58	-.58	-.45	-.60	-.58	-.57	-.57	-.55	-.45	.16	.31	.47	.56	NAE (b)
	.69	.56	.43	.30	.07	-.34	-.35	-.34	-.33	-.34	-.34	-.34	-.35	-.35	-.34	.04	.24	.38	.52	.63	NPL
60	.14	.23	.14	0	-.20	-.48	-.49	-.51	-.50	-.50	-.61	-.60	-.56	-.53	-.53	.15	.47	.64	.76	.83	City
	-.03	.24	.14	.01	-.16	-.41	-.42	-.43	-.43	-.43	-.53	-.50	-.47	-.47	-.45	.20	.53	.70	.84	.88	Bristol
	.22	.35	.17	-.04	-.12	-.44	-.43	-.45	-.44	-.44	-.51	-.51	-.49	-.44	-.41	.22	.49	.60	.69	.78	Monash
	.15	.28	.21	.07	-.12	-.38	-.39	-.39	-.41	-.39	-.53	-.49	-.46	-.44	-.41	.23	.51	.68	.81	.86	NAE (a)
	.18	.25	.19	.07	-.09	-.32	-.33	-.33	-.33	-.33	-.37	-.35	-.36	-.35	-.34	.23	.46	.62	.73	.78	NPL
75	-.79	-.58	-.25	-.19	-.25	-.35	-.38	-.38	-.37	-.41	-.59	-.56	-.52	-.49	-.48	.38	.64	.75	.78	.67	City
																					Bristol
																					Monash
	-.72	-.56	-.23	-.15	-.19	-.31	-.31	-.32	-.32	-.34	-.57	-.50	-.48	-.44	-.43	.40	.74	.84	.86	.74	NAE(a)
	-.75	-.46	-.16	-.12	-.18	-.30	-.31	-.31	-.31	-.32	-.48	-.43	-.42	-.41	-.48	.40	.64	.75	.78	.67	NPL
90	-.75	-.79	-.80	-.71	-.57		-.34	-.32		-.38		-.70	-.81		-.76	.57	.81	.87	.81	.56	City
	-.73	-.77	-.78	-.69	-.61	-.40	-.37	-.34	-.39	-.42	-.59		-.77	-.79	-.75	.50	.77	.84	.78	.54	Bristol
	-.70	-.75	-.69	-.62	-.55	-.34	-.32	-.32	-.34	-.34	-.55	-.62	-.69	-.74	-.70	.56	.75	.79	.75	.56	Monash
	-.68	-.74	-.73	-.61	-.49	-.33	-.28	-.28	-.28	-.33	-.49	-.61	-.73	-.74	-.68	.55	.82	.88	.82	.55	NAE (a)
	-.98	-1.01	-.81	-.77	-.66	-.50	-.45	-.45	-.43	-.56	-.65	-.81	-.90	-.99	-.96	.45	.73	.77	.75	.46	NAE (b)
	-.64	-.70	-.67	-.54	-.41	-.27	-.25	-.23	-.25	-.27	-.41	-.54	-.67	-.70	-.64	.52	.72	.77	.72	.52	NPL

TABLE 3

C.A.A.R.C. BUILDING MODEL STANDARD DEVIATION PRESSURE COEFFICIENT, $c\sigma_p = \frac{\sigma_p}{\frac{1}{2}\rho\bar{u}_H^2}$ (or $\frac{p'}{\frac{1}{2}\rho\bar{u}_H^2}$) AT $Z = (2/3)\,H$

Press. Tap / β	1	2	3	4	5	6	7	8	9	10	11	12	13	14	15	16	17	18	19	20	
0	.14	.14	.15	.15	.13	.16	.19	.18	.21	.23	.17	.14	.11	.13	.16	.23	.20	.25	.22	.20	Bristol
	.15	.18	.19	.18	.15	.22	.22	.23	.26	.27	.18	.17	.13	.17	.18	.26	.26	.23	.21	.22	Monash
			.20					.31					.15					.31			NAE (a)
			.22					.27					.11					.31			NAE (b)
	.13	.12	.13	.12	.13	.11	.16	.17	.18	.19	.09	.06	.05	.06	.09	.19	.18	.18	.16	.11	NPL
15																					Bristol
																					Monash
			.17					.37					.14					.17			NAE (a)
	.11	.14	.12	.12	.12	.05	.07											.26	.23	.19	NPL
30	.16	.16	.13	.12	.09	.06	.07	.07	.07	.09	.07	.06	.06	.06	.06	.05	.06	.15	.24	.24	Bristol
	.15	.14	.16	.12	.08	.07	.08	.07	.06	.08	.08	.07	.08	.06	.07	.08	.06	.18	.32	.24	Monash
			.15					.17					.10					.10			NAE (a)
																					NPL
45																					Bristol
																					Monash
			.12					.13					.09					.10			NAE (a)
	.12	.10	.08	.07	.07	0.004	.04											.09	.10	.13	NPL
60	.27	.11	.06	.06	.05	.06	.07	.06	.06	.07	.10	.07	.06	.06	.06	.09	.13	.13	.17	.18	Bristol
	.28	.12	.06	.06	.05	.06	.07	.07	.07	.06	.12	.07	.07	.07	.07	.10	.14	.13	.15	.18	Monash
			.09					.15					.10					.09			NAE (a)
																					NPL
75																					Bristol
																					Monash
			.30					.17					.15					.10			NAE (a)
	.22	.27	.19	.10	.08	.02	.04											.13	.13	.13	NPL
90	.22	.23	.25	.23	.23	.13	.11	.09	.11	.13	.23	.24	.25	.24	.23	.14	.16	.16	.17	.15	Bristol
	.22	.23	.23	.22	.25	.10	.08	.08	.10	.10	.26	.21	.22	.22	.22	.14	.15	.16	.14	.13	Monash
			.30					.18					.31					.12			NAE (a)
			.31					.10					.30					.22			NAE (b)
	.18	.20	.22	.20	.20	.08	.08		.08	.08	.20	.20	.22	.20	.18	.12	.13	.12	.13	.12	NPL

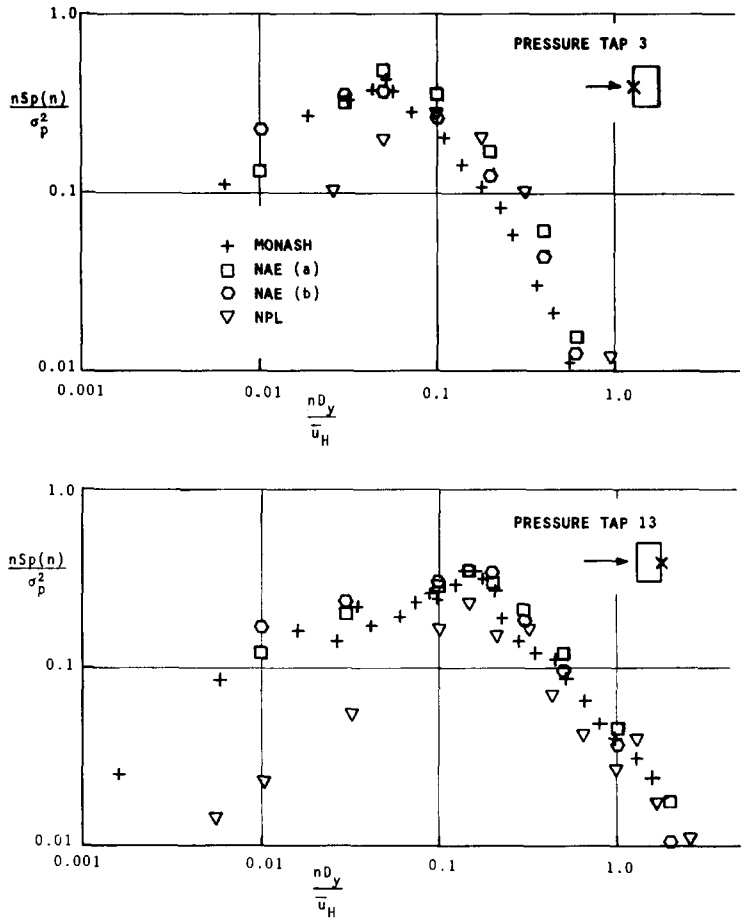

Fig.4. Pressure spectra measured on upstream and downstream faces, at centre $\frac{2}{3}H$, on the CAARC building model for $\beta = 0°$.

3.3 Response measurements

Aeroelastic models were tested at Monash University, NAE, NPL and The University of Western Ontario at length and velocity scales given in Table 1. All were linear mode models either pivoted at the base or mounted on a cantilever with an effective pivot about the base. The model response was measured as a base overturning moment via restoring force sensors and tip displacement obtained through static calibration, except for the NPL tests where only the standard deviation of tip displacement was determined from accelerometer measurements.

The mean and standard deviation of the x and y displacements at the top of the building as a function of reduced velocity for wind directions $\beta = 0$ and 90° and damping $\zeta = 0.01$ are given in Figs. 6 and 7. Two separately set-up

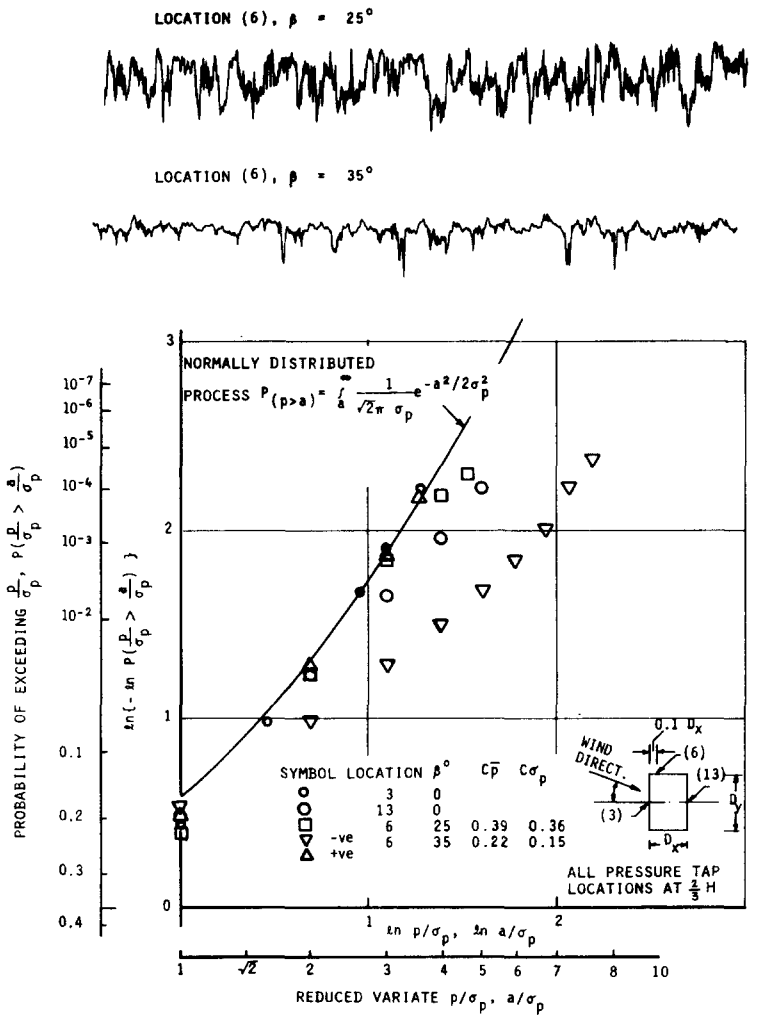

Fig.5. Probability distributions of pressure measurements on the surface of the CAARC building model (Monash).

and measured sets of data from Monash University are given (one set was measured as a student project), and two sets of data from the NAE are given for measurements in the two boundary layer models, refer to Table 1.

The majority of these response measurements compare within ±15%. Only very weak trends are observable. The scatter of data is a little more evident for $\beta = 0°$, which is understandable because of the effects of turbulence on rectangular sections with depth to upstream face ratios of about 2/3, when the separated shear layers are beginning to re-attach. At $\beta = 90°$, where the ratio of depth to upstream face is 3/2, the difference between the various response measurements is for the most part better than ±10%.

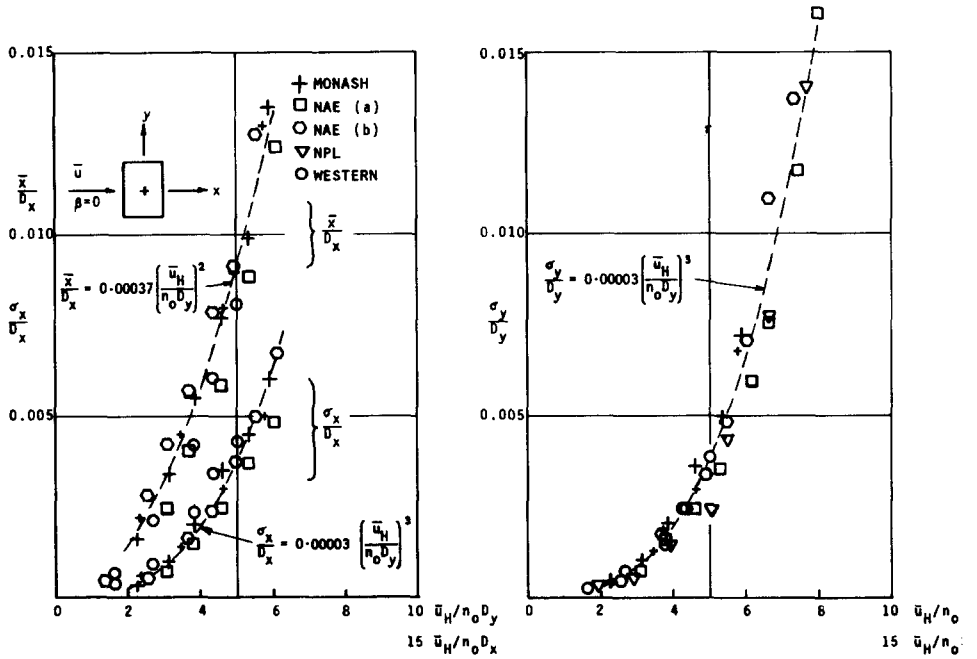

Fig.6. Displacement of the top of the CAARC building model as a function of reduced velocity for $\beta = 0$ and damping $\zeta = 0.01$.

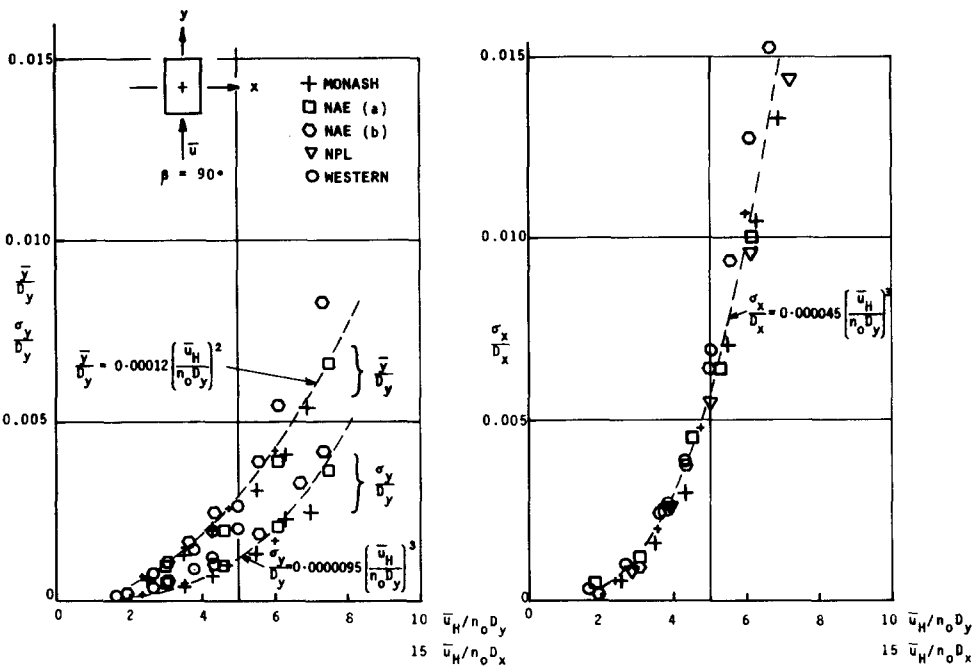

Fig.7. Displacement of the top of the CAARC building model as a function of reduced velocity for $\beta = 90°$ and damping $\zeta = 0.01$.

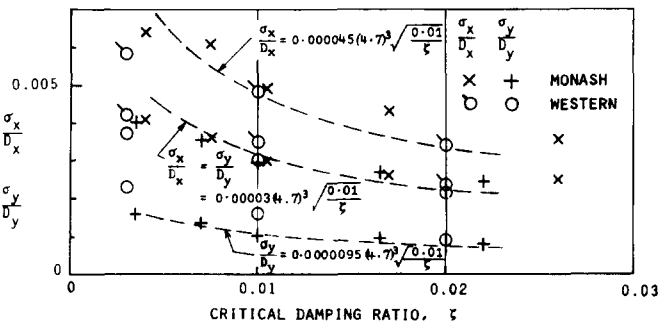

Fig.8. Effect of structural damping on the response of the CAARC building model at $\bar{u}_H/n_0D_y = 4.7$, $\bar{u}_H/n_0D_y = 7.0$.

The dashed curves shown in Figs. 6 and 7 have been included to assist in comparing other measurements with those reported here. These curves are not a best fit to the data in a mathematical sense, but rather have been fixed to vary with wind speed squared and cubed for the mean and standard deviation measurements, respectively, with the constant in each case selected to give the best fit to the majority of the data, (i.e. values a long way from the majority have been ignored in determining the constants). Whilst the variation of mean response with the square of the wind speed may come as no surprise, the fit of the standard deviation of response to the cube of the wind speed is slightly illusory. In fact, the standard deviation of response tends to vary with wind speed to a lower power than three at low reduced velocities and to a higher power than three at the higher reduced velocities approaching the peak of the force spectrum.

A comparison of the effects of change in structural damping was possible between the Monash University and University of Western Ontario data and this is given in Fig.8. Both sets of data appear to have inconsistencies, at low values of damping in particular, but there are no obvious trends. Holmes noted that difficulties were encountered in measuring the damping at low values because of cross-coupling effects. All results presented show dependence of response to an inverse exponent of damping close to a half, as shown by the dashed curves fitted in Fig.8.

The effect of wind direction on response is shown in Fig.9, where the mean and standard deviation of the base overturning moments have been presented for a value of $u_H/n_0D_y = 4.7$, $(u_H/n_0D_x = 7.0)$. The problem in presenting these data is in the selection of normalising lengths. In this case, base overturning moments in the positive x and y directions have been defined as M_x and M_y, respectively, and mean and standard deviations of moments in both x and y directions ($\bar{M}_x \bar{M}_y$, σ_{M_x}, σ_{M_y}) have all been normalised by $\frac{1}{2}\rho\bar{u}_H^2H^2D_y$, i.e.

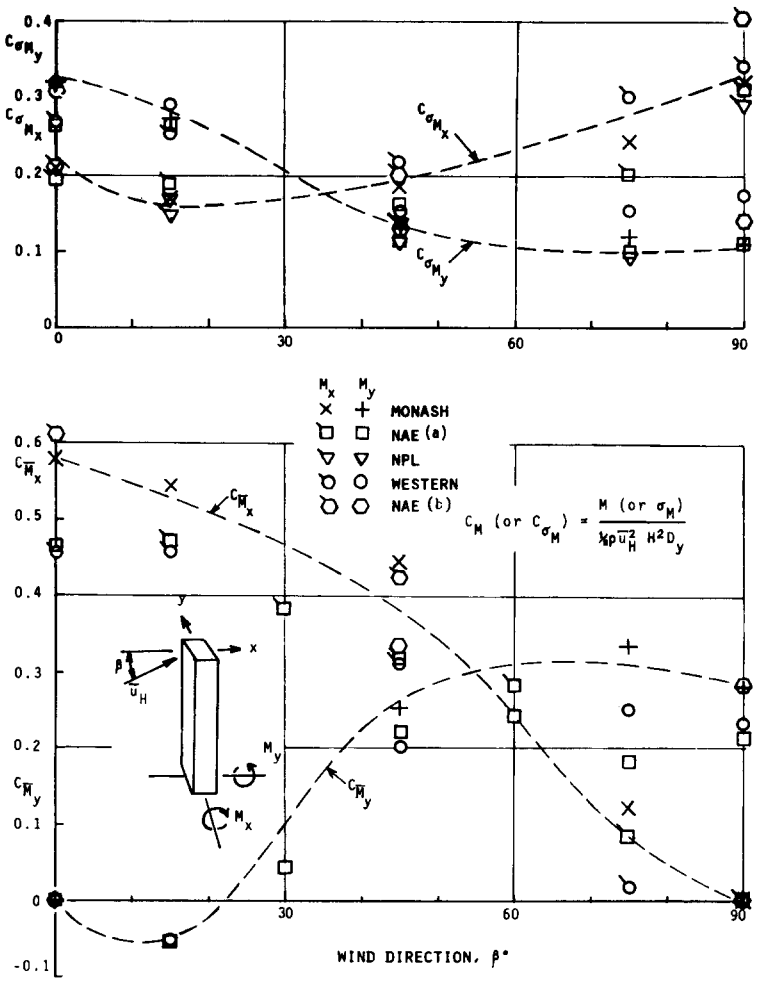

Fig.9. Base overturning moments as a function of wind direction for the CAARC building model at $\bar{u}_H/n_0 D_y = 4.7$, $\zeta = 0.01$.

$$C_{M_x} = \frac{\overline{M}_x}{\frac{1}{2}\rho \bar{u}_H^2 H^2 D_y}$$

$$C_{\overline{M}_y} = \frac{\overline{M}_y}{\frac{1}{2}\rho \bar{u}_H^2 H^2 D_y}$$

$$C_{\sigma_{M_x}} = \frac{\sigma_{M_x}}{\frac{1}{2}\rho \bar{u}_H^2 H^2 D_y}$$

$$C_{\sigma_{M_y}} = \frac{\sigma_{M_y}}{\frac{1}{2}\rho \bar{u}_H^2 H^2 D_y}$$

The base overturning moment data can be presented in terms of displacement and vice versa. For a constant density, linear mode, building the relationship can be developed as follows:
The fundamental natural frequency, n_0, of the constant density linear mode building can be expressed as

$$n_0 = (1/2\pi)\sqrt{T/I} \tag{1}$$

where I is the mass moment of inertia about the base, and T is the rotation stiffness of the building about the base. For a tall building, the moment of inertia may be approximated as

$$I = \tfrac{1}{3}\rho_s H^3 D_x D_y \tag{2}$$

where ρ_s is the density of the building. The base overturning moment, M, in terms of a tip displacement, Δ, is

$$M = T\,\Delta/H \tag{3}$$

which on substitution from (1) and (2) gives

$$M = \tfrac{1}{3}(2\pi n_0)^2 \cdot \rho_s H^2 D_x D_y \cdot \Delta \tag{4}$$

Evaluating for the CAARC Building Model gives

$$C_{M_x} = 3510 \left(\frac{D_x}{D_y}\right)^2 \left(\frac{n_0 D_y}{u_H}\right)^2 \left(\frac{x}{D_x}\right)$$

$$C_{M_y} = 3510 \left(\frac{D_x}{D_y}\right) \left(\frac{n_0 D_y}{\bar{u}_H}\right)^2 \left(\frac{y}{D_y}\right) \tag{5}$$

and similarly $C_{M_{\sigma_x}}$ and $C_{M_{\sigma_y}}$.

The comparison of measurements of base overturning moment or tip deflection with wind direction shows the poorest agreement between the sets of data. The author believes that the cause of the differences may lie in the behaviour of the shear layers and attendant re-attachment, which is known to be dependent on the incident flow turbulence and even acoustic energy in the wind tunnel. These effects on shear layer behaviour become more apparent when the flow direction is almost normal to a main face.

The dashed curves shown in Fig. 9, whilst being consistent with the earlier curves at $\beta = 0$ and 90°, have been drawn through the data only to assist in reading the figure.

Some response spectra were measured at Monash University and the NAE, but direct comparison was not possible because the data were not measured at the same values of reduced velocity. The response spectra measured at Monash University have already been published in the form of a generalised force spectrum by Saunders and Melbourne [6] and the measurements at the NAE are to be published.

4. Conclusions

The comparison of pressure and response measurements on the CAARC Building Model tested at six establishments, in simulated wind flows, showed only small differences mostly within the scatter of reasonable experimental accuracy.

Small trends were observable in respect of pressure measurements which could be attributed to differences in the approaching longitudinal velocity spectrum and to the requirement for blockage corrections. There were no obvious trends in the dynamic response measurements and the majority of these data compared within ±15%.

It might have been more interesting, in addition, to have compared data measured in incorrectly modelled wind flows, and perhaps this could be taken up by subsequent investigators.

Acknowledgements

Approval to use data supplied by the contributors listed in section 1 and their assistance in checking the data as finally presented is gratefully acknowledged.

Thanks are also due to the CAARC Aerodynamics Coordinators, in particular Messrs Wardlaw and Moss, for conceiving and initiating the idea of testing a standard building model in a number of boundary layer wind tunnels.

Notation

C_M base overturning moment coefficient $= \left(\dfrac{M}{\frac{1}{2}\rho \bar{u}_H^2 H^2 D_y}\right)$

D_x narrow dimension of building cross section = 100 ft (30.5 m)

D_y wide dimension of building cross section = 150 ft (45.7 m)

H building height = 600 ft (182.9 m)

M_x base overturning moment in the x direction

M_y base overturning moment in the y direction

n frequency

n_0 natural fundamental frequency of the building (0.2 Hz in x and y direction)

p local pressure

p_H reference static pressure at height H

$S_p(n)$ power spectral density of pressure fluctuations

$S_u(n)$ power spectral density of velocity fluctuations

$\bar{u}$ local mean longitudinal velocity

$\bar{u}_H$ reference velocity at height H

z height above ground

α exponent in power-law representation of velocity profile (see Fig.2)

β wind angle (see Fig. 1)
σ_p standard deviation or root-mean-square value of pressure fluctuations
σ_u standard deviation or root-mean-square value of the longitudinal velocity fluctuation
ρ air density
ζ critical damping ratio

References

1 R.L. Wardlaw and G.F. Moss, A standard tall building model for the comparison of simulated natural winds in wind tunnels, C.A.A.R.C., C.C.662m Tech.25, January 1970.
2 J.D. Holmes, Aeroelastic tests on the C.A.A.R.C. standard building model, Boundary Layer Wind Tunnel Report BLWT-1-75, University of Western Ontario, Canada, August 1975.
3 D.E. Walshe, Tests on the standard tall building proposed by the Commonwealth Advisory Aeronautical Research Council, NPL Report Mar Sc R120, September 1974.
4 J.A.B. Wills and P. Jones, Measurements of pressure fluctuations on a model of the C.A.A.R.C. standard tall building, NPL Report Mar Sci R115, May 1974.
5 R.J. McKeon and W.H. Melbourne, Wind tunnel blockage effects and drag on bluff bodies in a rough wall boundary layer, Proc. 3rd Int. Conf. on Wind Effects on Buildings and Structures, Saikon, Tokyo, 1971, pp. 263—272.
6 J.W. Saunders and W.H. Melbourne, Tall rectangular building response to cross-wind excitation, Proc. 4th Int. Conf. on Wind Effects on Buildings and Structures, Heathrow, Cambridge University Press, London, 1975, pp. 369—380.